Journal of Hydrology 530 (2015) 484–499

Contents lists available at ScienceDirect

Journal of Hydrology

journal homepage: www.elsevier.com/locate/jhydrol

Well hydrograph analysis for the characterisation of flow dynamics and conduit network geometry in a karst aquifer, Bükk Mountains, Hungary

Attila Kovács [a,c,*], Pierre Perrochet [b], Enikő Darabos [c,d], László Lénárt [d], Péter Szűcs [c,d]

[a] Geological and Geophysical Institute of Hungary, 14 Stefania út, Budapest H-1143, Hungary
[b] CHYN, University of Neuchâtel, Rue Emile-Argand 11, CH-2007 Neuchâtel, Switzerland
[c] MTA-ME Research Group of Geoengineering, Miskolc-Egyetemváros 3515, Hungary
[d] University of Miskolc, Department of Hydrogeology and Engineering Geology, Miskolc-Egyetemváros 3515, Hungary

ARTICLE INFO

Article history:
Received 13 April 2015
Received in revised form 16 September 2015
Accepted 22 September 2015
Available online 30 September 2015
This manuscript was handled by Andras Bardossy, Editor-in-Chief, with the assistance of Wolfgang Nowak, Associate Editor

Keywords:
Karst
Well hydrograph
Hydrograph analysis
Conduit network
Szinva spring
Garadna spring

SUMMARY

The present paper introduces new well hydrograph analytical tools for parameter estimation in karst aquifers. The analytical formulae provided in this study link aquifer properties with hydrograph recession coefficients, and provide quantitative characterisation of the spatial and temporal variations of the water table. Generally, spring hydrograph analytical techniques provide information on the characteristic hydraulic parameters and conduit spacing in a karstic catchment, while well hydrograph analysis provides information on local hydraulic and geometric properties of individual matrix blocks and in certain cases on the deep unkarstified aquifer zone.

The combination of the spring and well hydrograph analytical methods represents a useful tool for understanding the structure and hydraulic behaviour of karst systems.

A new well hydrograph analytical approach is presented, which makes the estimation of conduit spacing and catchment geometries possible. In most cases well hydrograph peaks can be decomposed into three exponential segments. Exponential segments in shallow systems do not correspond to different types of storage, but in most cases originate from the emptying of fissured matrix blocks.

The proposed parameter estimation method is demonstrated through the application of field data. The test site is located in the Bükk Mountains, Hungary. Analytical methods were applied on two adjacent karstic catchments feeding the Szinva and Garadna springs. Hydrograph analysis of both springs and three well hydrographs were performed to investigate the hydraulic behaviour of the karst system and to estimate the spatial geometry of karst conduits. According to hydrograph analytical results, both spring and well hydrographs indicated similar matrix block geometries. Hydrograph analysis revealed the change of flow scale indicated by a significant drop of the value of recession coefficient.

The investigation method introduced in this study provides important information for water resource assessment, contamination risk assessment, vulnerability assessment, flood prediction, geotechnical and speleological studies.

1. Introduction

To understand the hydraulic functioning of karst systems, and to be able to construct reasonable groundwater flow models, information on hydraulic properties and on conduit network geometry are essential (Király and Morel, 1976; Király, 2002; Kovács, 2003a, 2003b; Worthington, 2009). Insufficient data on conduit network geometry entails difficulties in the characterisation and groundwater modelling of karst hydrogeological systems. Generally, very limited information on hydraulic properties and the geometry of the conduit system are available through the application of traditional investigation techniques: Classical geological and hydrogeological investigations, speleological and geophysical observations, hydraulic tests and tracing experiments provide limited information on the spatial geometry and hydraulic properties of hydraulically active karst conduits. However, in most cases well hydrograph data, coupled with information on the hydraulic properties of the low-permeability rock matrix are available or obtainable. Hydrograph analytical techniques presented here are suitable for estimating effective hydraulic parameters and geometric characteristics of karst systems.

* Corresponding author at: Geological and Geophysical Institute of Hungary, 14 Stefania út, Budapest H-1143, Hungary.
E-mail address: kovacs.attila@mfgi.hu (A. Kovács).

http://dx.doi.org/10.1016/j.jhydrol.2015.09.058
0022-1694/© 2015 Published by Elsevier B.V.

The primary goal of the present paper is to outline the theoretical bases of quantitative well hydrograph analysis, and to provide field examples for the combined application of the spring and well hydrographs analytical techniques introduced by Kovács (2003a), Kovács et al. (2005), Kovács and Perrochet (2008) and Kovács and Perrochet (2014).

2. Precedents

Spring hydrograph analytical methods for parameter estimation were provided by several authors (Rorabaugh, 1964; Berkaloff, 1967; Bagarić, 1978; Kovács, 2003a, 2003b; Kovács, et al., 2005; Kovács and Perrochet, 2008). Spring hydrograph analytical methods for the estimation of conduit network geometry were discussed by Kovács (2003a), Kovács et al. (2005) and Kovács and Perrochet (2008).

The hydraulic behaviour of karst systems is primarily determined by the spatial geometry of karst conduits, the diameter of karst conduits, and the hydraulic properties of the low-permeability matrix. While conduit diameter plays an important role during flood recession, it has limited influence on groundwater flow during baseflow recession (Kovács, 2003a; Kovács, et al., 2005).

As a consequence, the hydraulic properties of karst conduits are reflected in spring discharge during flood events, while conduit network geometry and matrix hydraulic properties can be determined from hydrographs during baseflow periods.

Well hydrograph analysis for the estimation of hydraulic properties in karst was applied by Rorabough (1960), Atkinson (1977), Shevenell (1996), Powers and Shevenell (2000). It was assumed by Shevenell (1996) that exponential components of well hydrographs represent three types of storage upgradient of the monitored point. This assumption will be further discussed in this study. The mathematical derivation of two-dimensional well hydrograph formulae together with detailed numerical analyses were provided by Kovács and Perrochet (2014).

The present paper introduces new analytical parameter estimation tools, and provides a methodology for the application of well hydrograph data for parameter estimation in karst aquifer systems. The introduced methodology is demonstrated through a detailed field study.

3. Goals and methodology

The primary goal of the present paper is to introduce a quantitative method for the estimation of hydraulic parameters and conduit network geometry of karst aquifers based on well hydrograph analysis in order to facilitate the parameter estimation and distributive groundwater flow modelling of karst hydrogeological systems and to gain insight into their hydraulic functioning.

For the purpose of this study, a simple conceptual model of karst and connected water systems has been applied. Analytical solutions for the spatial–temporal variation of hydraulic potentials within two-dimensional rectangular blocks representing matrix volumes in karst aquifers were developed. Parameter estimation tools based on these analytical solutions together with field applications of well and spring hydrograph analyses are provided in this study.

Spring and well hydrograph data collected from a test site were analysed. Individual hydrograph peaks and master recession curves were decomposed using new analytical techniques. Spring and well hydrograph data were compared, and conduit network geometric parameters were estimated. The obtained results were compared and verified through field observations.

The applied methodology led to significant findings about the hydraulic functioning of the karst system investigated in this study and of karst hydrodynamics in general.

4. Conceptual model

A simple conceptual model of karst and connected water systems was defined by Kovács (2003a) and Kovács et al. (2005). This model consists of a rectangular karstic catchment, a regular network of karst conduits embedded in rock matrix, and a single outlet (spring) which drains the entire conduit network. The characteristic parameters of such model include the hydraulic parameters of the rock matrix and of the conduit system, spacing of karst conduit, and the spatial extent of the catchment. This conceptual model has been modified to include well hydrographs, and the updated model was applied in this study (Fig. 1).

It was shown by Kovács (2003a) and Kovács et al. (2005) that there is a fundamental difference in hydraulic behaviour between karst and fractured systems depending on their degree of heterogeneity which can be quantified by a combination of hydraulic and geometric properties.

The baseflow discharge of well-developed karst systems is controlled by the drainage of individual matrix blocks. This flow condition was referred to as Matrix-Restricted Flow Regime (MRFR).

Besides the hydraulic properties of the rock matrix and fracture spacing, the baseflow discharge of fractured systems is also influenced by the hydraulic parameters of fractures/conduits, and the extent of the entire catchment. This flow condition was defined as Conduit-Influenced Flow Regime (CIFR).

A threshold value for conduit conductance between these two domains can be expressed as follows (Kovács, 2003a; Kovács, et al., 2005) (Fig. 2):

$$K_c^* \approx 3\pi^2 T_m A f \quad (1)$$

where T_m [$L^2\,T^{-1}$] is matrix transmissivity, K_c [$L^3\,T^{-1}$] is 1D conduit conductance, A [L^2] is aquifer extent, f [L^{-1}] is average conduit frequency.

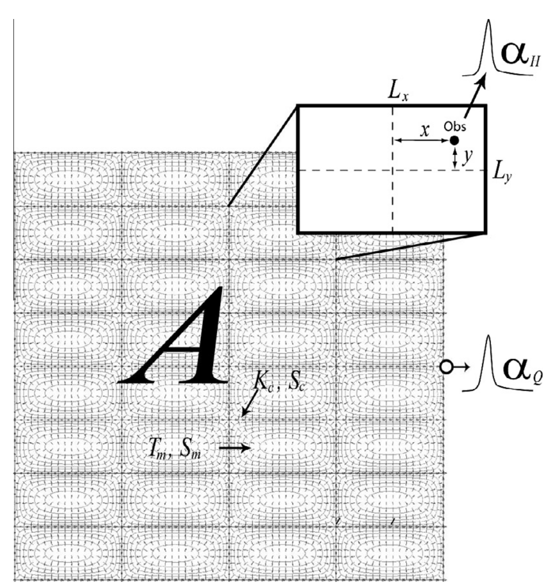

Fig. 1. A simple conceptual model suitable for the quantitative characterisation of karst hydrogeological systems. T_m [$L^2\,T^{-1}$] transmissivity of the low-permeability matrix, S_m [–] storativity of the low-permeability matrix, K_c [$L^3\,T^{-1}$] 1D conduit conductance, S_c [L] 1D conduit storativity, A [L^2] spatial extent of the aquifer, L_x and L_y [L] block size, x and y distance of piezometer from block centre, α_Q spring hydrograph recession coefficient, α_H well hydrograph recession coefficient. After Kovács et al. (2005).

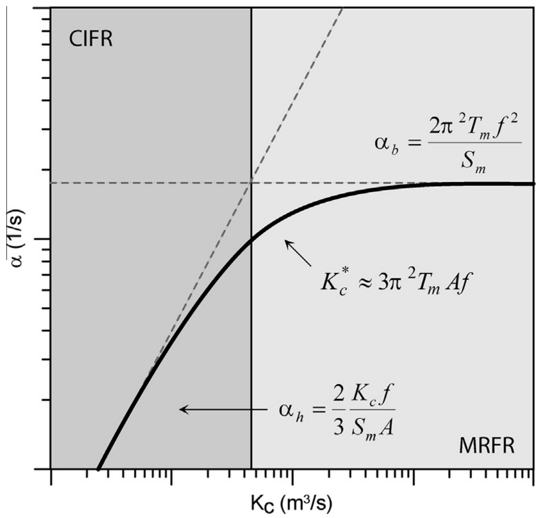

Fig. 2. Dependence of the baseflow recession coefficient on conduit conductance. $K_c{}^*$ is the threshold value between MRFR and CIFR baseflow. From Kovács et al. (2005).

The analytical formulae presented in this paper are valid for karst systems (MRFR regime) where $K_c > K_c{}^*$.

5. Recession coefficient

Recession coefficient is the main hydrograph parameter used in this study. The notion of the recession coefficient was first introduced by Maillet (1905). Maillet's interpretation is based on the drainage of a prismatic reservoir, and presumes that spring discharge is a linear function of the volume of water held in storage:

$$Q = \alpha V \tag{2}$$

where Q is discharge [$L^3\,T^{-1}$], V is volume of water in the reservoir [L^3], α is recession coefficient [T^{-1}] usually expressed in days. Under recession conditions, discharge also corresponds to the decrease of storage water:

$$Q = -\frac{dV}{dt} \tag{3}$$

Eqs. (2) and (3) and integrating during the recession time yield the Maillet formula:

$$Q_{(t)} = Q_0 e^{-\alpha t} \tag{4}$$

where Q_0 is the flow rate at the start of the recession period.

Assuming that the volume of water held in storage is a linear function of the reservoir area A and the water level H prevailing in it (i.e. $V = AH$), it can easily be shown that this level also follows an exponential behaviour with the same recession coefficient, namely:

$$H_{(t)} = H_0 e^{-\alpha t} \tag{5}$$

where H_0 is the head at the start of the recession period.

It is demonstrated above that recession coefficient can equally be expressed from discharge and hydraulic head time series data.

6. Analytical solutions

6.1. Hydraulic head distribution in an asymmetric block

The distribution of hydraulic heads in the matrix blocks of a karst system during recession is strongly time dependent; primarily influenced by the geometry and hydraulic properties of the blocks. Initial head distribution (as a consequence of groundwater recharge) over the blocks influences the recession process at early times, and has negligible influence on the recession curve on the longer term (Kovács and Perrochet, 2008). A new analytical solution describes the spatio-temporal distribution of hydraulic heads over a 2-dimensional (2D) matrix block during a recession period. This solution (Eq. (6)) involves a uniform initial head distribution assumption over the blocks.

$$H_{(x,y,t)} = \frac{16H_0}{\pi^2}\sum_{m=0}^{\infty}\frac{(-1)^m\cos\left((2m+1)\frac{\pi}{L_x}x\right)}{(2m+1)}e^{-a(2m+1)^2} \times \sum_{n=0}^{\infty}\frac{(-1)^n\cos\left((2n+1)\frac{\pi}{L_y}y\right)}{(2n+1)}e^{-a\beta^2(2n+1)^2} \tag{6}$$

where

$$a = \frac{\pi^2 Tt}{SL_x^2} \text{ and } \beta = \frac{L_x}{L_y}$$

where T [$L^2\,T^{-1}$] is block transmissivity, S [–] is block storativity, L_x and L_y [L] are block size, β [–] is asymmetry factor ($\beta = L_x/L_y$), x and y are distances of the observation well from block centre.

Uniform hydraulic head was assumed as boundary condition along the sides of the rectangular blocks representing karst conduits, and the initial condition comprises uniform hydraulic head of H_0 [L] over the block surface. This solution was written down as the product, in the x and y directions, of the 1D solution given in Carslaw and Jaeger (1959). It follows from Eq. (6) that:

$$H_{(x,y,t)} = \frac{16H_0}{\pi^2}\left(\cos\left(\frac{\pi x}{L_x}\right)e^{-a} - \frac{1}{3}\cos\left(\frac{3\pi x}{L_x}\right)e^{-9a} + \frac{1}{5}\cos\left(\frac{5\pi x}{L_x}\right)e^{-25a} - \ldots\right) \left(\cos\left(\frac{\pi y}{L_y}\right)e^{-a\beta^2} - \frac{1}{3}\cos\left(\frac{3\pi y}{L_y}\right)e^{-9a\beta^2} + \frac{1}{5}\cos\left(\frac{5\pi y}{L_y}\right)e^{-25a\beta^2}\ldots\right) \tag{7}$$

Leading to the expansion:

$$H_{(x,y,t)} = \frac{16H_0}{\pi^2}\left(\begin{array}{l} \cos\left(\frac{\pi x}{L_x}\right)\cos\left(\frac{\pi y}{L_y}\right)e^{-a(1+\beta^2)} - \frac{1}{3}\cos\left(\frac{\pi x}{L_x}\right)\cos\left(\frac{3\pi y}{L_y}\right)e^{-a(1+9\beta^2)} + \frac{1}{5}\cos\left(\frac{\pi x}{L_x}\right)\cos\left(\frac{5\pi y}{L_y}\right)e^{-a(1+25\beta^2)} \\ -\frac{1}{3}\cos\left(\frac{3\pi x}{L_x}\right)\cos\left(\frac{\pi y}{L_y}\right)e^{-a(9+\beta^2)} + \frac{1}{9}\cos\left(\frac{3\pi x}{L_x}\right)\cos\left(\frac{3\pi y}{L_y}\right)e^{-9a(1+\beta^2)} \\ -\frac{1}{15}\cos\left(\frac{3\pi x}{L_x}\right)\cos\left(\frac{5\pi y}{L_y}\right)e^{-a(9+25\beta^2)} + \frac{1}{5}\cos\left(\frac{5\pi x}{L_x}\right)\cos\left(\frac{\pi y}{L_y}\right)e^{-a(25+\beta^2)} \\ -\frac{1}{15}\cos\left(\frac{5\pi x}{L_x}\right)\cos\left(\frac{3\pi y}{L_y}\right)e^{-a(25+9\beta^2)} + \frac{1}{25}\cos\left(\frac{5\pi x}{L_x}\right)\cos\left(\frac{5\pi y}{L_y}\right)e^{-25a(1+\beta^2)}\ldots \end{array}\right) \tag{8}$$

Fig. 3 indicates the first nine hydrograph components ($n = m = 2$ in Eq. (6)) for a virtual observation point.

As shown in Eq. (8), the baseflow hydrograph is not exactly exponential, but it can be described as a superposition of an infinite number of exponential components. According to Fig. 3,

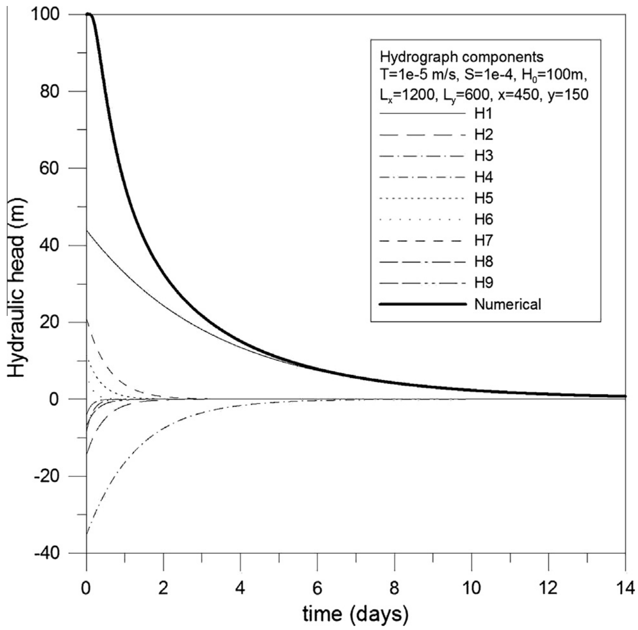

Fig. 3. Analytical well hydrograph components for an observation point ($T = 1e{-}5\ m^2/s$, $S = 1e{-}4$, $H_0 = 100$ m, $L_x = 1200$, $L_y = 600$ m, $x = 450$, $y = 150$). Numerical values were simulated using a 2D finite element model.

or

$$\alpha_2 = \frac{\pi^2 T}{S L_x^2}(9 + \beta^2) = \frac{\pi^2 T}{S}\left(\frac{9}{L_x^2} + \frac{1}{L_y^2}\right) \quad \text{for } L_x > L_y \tag{11}$$

The third exponential can be expressed as:

$$\alpha_3 = \frac{\pi^2 T}{S L_x^2}(1 + 25\beta^2) = \frac{\pi^2 T}{S}\left(\frac{1}{L_x^2} + \frac{25}{L_y^2}\right) \quad \text{for } L_y > L_x \tag{12}$$

or

$$\alpha_3 = \frac{\pi^2 T}{S L_x^2}(25 + \beta^2) = \frac{\pi^2 T}{S}\left(\frac{25}{L_x^2} + \frac{1}{L_y^2}\right) \quad \text{for } L_x > L_y \tag{13}$$

6.2. Hydraulic head distribution in a symmetric block

A symmetric approximation of block shape (square blocks) can be applied in the case of negligible anisotropy with quasi-symmetric matrix blocks. This solution is also useful when only the "baseflow" recession coefficient (α_1) can be estimated because of insufficient or bad quality data. In such cases block asymmetry (β) cannot be calculated, and thus the application of the asymmetric solution would be problematic.

The following new symmetric solution provides an efficient tool for parameter estimation is these situations. For symmetric blocks, Eq. (8) takes the following form ($n = m = 2$):

$$H = \frac{16H_0}{\pi^2}\left(\begin{array}{l} \cos\left(\frac{\pi x}{L}\right)\cos\left(\frac{\pi y}{L}\right)e^{-2a} - \frac{1}{3}\left[\cos\left(\frac{\pi x}{L}\right)\cos\left(\frac{3\pi y}{L}\right) + \cos\left(\frac{3\pi x}{L}\right)\cos\left(\frac{\pi y}{L}\right)\right]e^{-10a} \\ + \frac{1}{5}\left[\cos\left(\frac{\pi x}{L}\right)\cos\left(\frac{5\pi y}{L}\right) + \cos\left(\frac{5\pi x}{L}\right)\cos\left(\frac{\pi y}{L}\right)\right]e^{-26a} + \frac{1}{9}\cos\left(\frac{3\pi x}{L}\right)\cos\left(\frac{3\pi y}{L}\right)e^{-18a} \\ - \frac{1}{15}\left[\cos\left(\frac{3\pi x}{L}\right)\cos\left(\frac{5\pi y}{L}\right) + \cos\left(\frac{5\pi x}{L}\right)\cos\left(\frac{3\pi y}{L}\right)\right]e^{-34a} + \frac{1}{25}\cos\left(\frac{5\pi x}{L}\right)\cos\left(\frac{5\pi y}{L}\right)e^{-50a} \end{array}\right) \tag{14}$$

similarly to spring hydrographs (Kovács and Perrochet, 2008), only three exponential components contribute visibly to the total hydrograph, while the others disappear at early times of the recession process. For any asymmetric block, the first component is H1, the second component is H2 (for $L_y > L_x$) or H4 (for $L_y < L_x$), where H2 = H4 in the block centre of symmetric blocks ($L_x = L_y$ and $x = y = 0$). The third component is H3 (for $L_y > L_x$) or H7 (for $L_y < L_x$).

This explains why most hydrographs can be decomposed into three exponential components only.

It was assumed by Shevenell (1996) that exponential components of well hydrographs represent three types of storage upgradient of the monitored point, similarly to the spring hydrograph decomposition theory of Forkasiewicz and Paloc (1967). According to the above analytical solution, at least three significant exponential components appear on the well hydrograph of a homogeneous block, and the assumption of several storages is unnecessary to explain hydrograph components.

Based on Eq. (8) the recession coefficient of the first exponential component can be expressed as follows:

$$\alpha_1 = \frac{\pi^2 T}{S L_x^2}(1 + \beta^2) = \frac{\pi^2 T}{S}\left(\frac{1}{L_x^2} + \frac{1}{L_y^2}\right) \tag{9}$$

And the second exponential can be expressed as:

$$\alpha_2 = \frac{\pi^2 T}{S L_x^2}(1 + 9\beta^2) = \frac{\pi^2 T}{S}\left(\frac{1}{L_x^2} + \frac{9}{L_y^2}\right) \quad \text{for } L_y > L_x \tag{10}$$

It follows from Eq. (14) that "baseflow" recession coefficient can be expressed from the first exponential component as:

$$\alpha_1 = \frac{2\pi^2 T}{S L^2} \tag{15}$$

While subsequent exponentials can be expressed as:

$$\alpha_2 = \frac{10\pi^2 T}{S L^2} \tag{16}$$

$$\alpha_3 = \frac{18\pi^2 T}{S L^2} \tag{17}$$

Consequently, the "baseflow" sections of well hydrographs can be used for estimating block size (if block hydraulic parameters are known), or hydraulic diffusivity of matrix blocks (if block size is known) of a karst system. Most importantly, hydrograph analysis represents an additional tool for verifying assumptions on the geometric and hydraulic parameters of complex hydrogeological systems.

According to Eqs. (9–12) and (15–17), similar formulae can be used for expressing recession coefficients from well hydrographs as from spring hydrographs (Kovács et al., 2005; Kovács and Perrochet, 2008). However, the former represents individual block properties, the latter one provides information on the average block properties within a karstic catchment.

7. Test site

Our test site, which includes the Szinva and Garadna spring catchments is located in the Bükk Mountains in Northern Hungary (Fig. 4).

The Bükk Mountains consist of karstified platform facies Triassic limestone with marl, clay and chert intercalations. Jurassic slates and Cretaceous volcanites (diabase, gabbro and metabasalt) are also present in large extents on the surface in the western and south-western part of the mountain. Triassic limestones of the Bükk constitute a deep karst water reservoir which extends several thousand metres below the surface. About two dozen karst springs and thermal wells can be found at the rim of the mountain and the surrounding area, yielding tepid or warm thermal waters. In the deep reservoir water temperature is between 30 and 100 °C.

Scientific investigation of hydrochemical characteristics of the thermal springs of the Bükk area started in 1762 (Dombi, 1766). The first karst hydrogeological field investigations were started by Kessler (1955, 1959). Aspects of the hydrogeological characteristics of the Bükk area were studied by Sásdi et al. (2002), Pelikán (2005), Lénárt (2005, 2010), Lénárt et al. (2014), Gondár-Sőregi et al. (2011), Darabos (2010), Darabos et al. (2012).

The installation of monitoring bores in the Bükk started in 1983 (Böcker, 1969; Böcker and Vecsernyés, 1983). The groundwater monitoring program which includes the continuous registration of water levels in monitoring bores, caves and karst springs was launched in 1992. The monitoring network which is operated by the University of Miskolc, currently includes 34 monitoring stations and collected data from 80 different locations (Lénárt et al., 2014). Most stations register water levels, while temperature and electrical conductivity data are also being collected at several stations at 15–60 min sampling frequency. The monitoring bores are equipped with DATAQUA type pressure sensors Dataqua (2002). Pressure, temperature and conductivity data is continuously transferred to a distant PC via DATAQUA DA23 GSM communication units. No comprehensive analysis of the accumulated database has been undertaken to date, and thus the present study represents an important step towards the hydrological understanding of the study area.

7.1. The Szinva catchment

The Szinva catchment extends over a 12 × 3 km elongated area of 37 km^2 (Fig. 4). The catchment was delineated based on surface topography, tracing experiments and water budget calculations (Hernádi et al., 2013). The Szinva catchment covers most of the Fennsík (uplands) area of the Bükk Mountains. The geology of the uplands zone includes middle- and upper-Triassic limestones. The majority of the area is hosted by the Bükkfennsík Formation (anchimetamorhosed platform facies limestone). The southern strip of the catchment consists of the Felsőtárkányi Formation (intrashelf basin facies thick bedded limestone with marl and chert intercalations), while the northern strip is made up of the Fehérkői Formation (thick-bedded platform facies limestone) (Figs. 4 and 5).

The uplands area has a large number of sinkholes (Hernádi et al., 2013). According to the spatial analysis undertaken within the frameworks of the present study, sinkholes are not spread randomly over the area, but follow linear features supposedly indicating the location of karst conduits. It is evidenced in the neighbouring Sebesvizi catchment, that cave branches extend

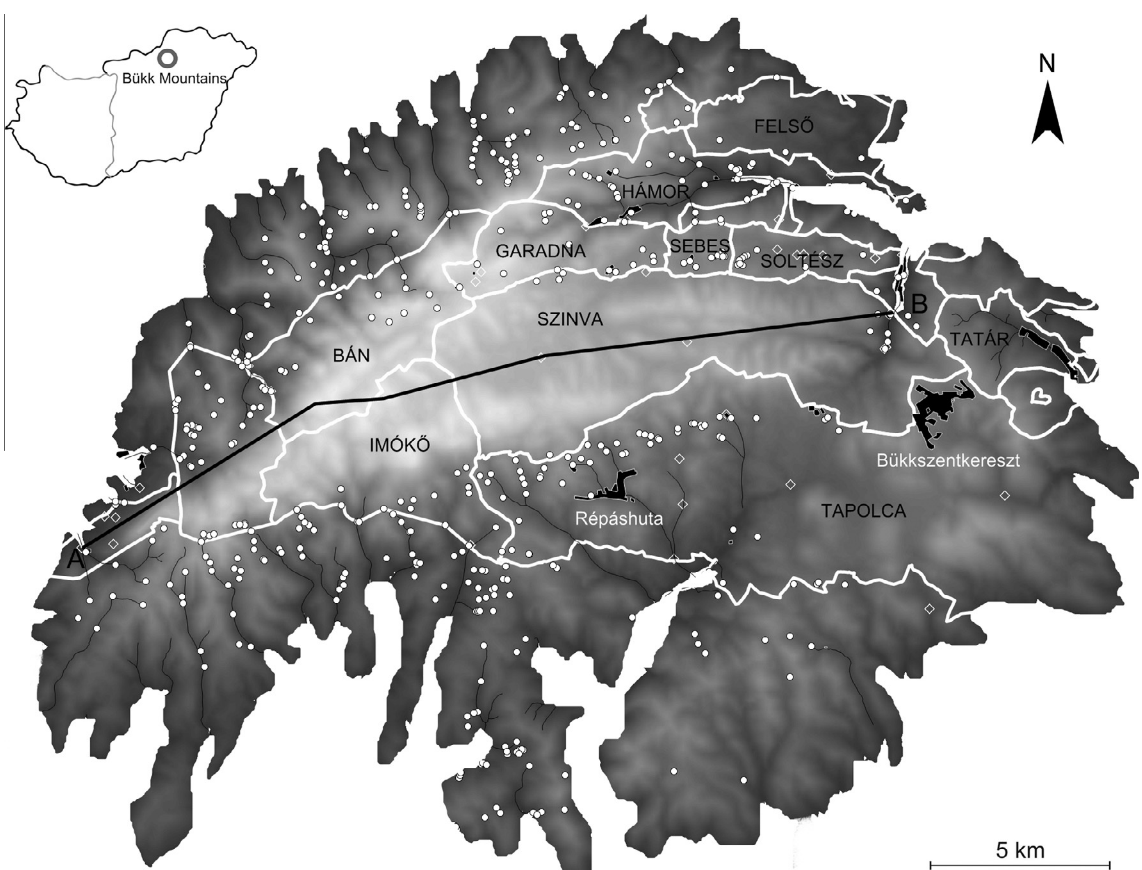

Fig. 4. Test site topography. White lines indicate catchment boundaries, white dots indicate karst springs, and diamonds indicate observation wells. Black line indicates A–B cross sectional line.

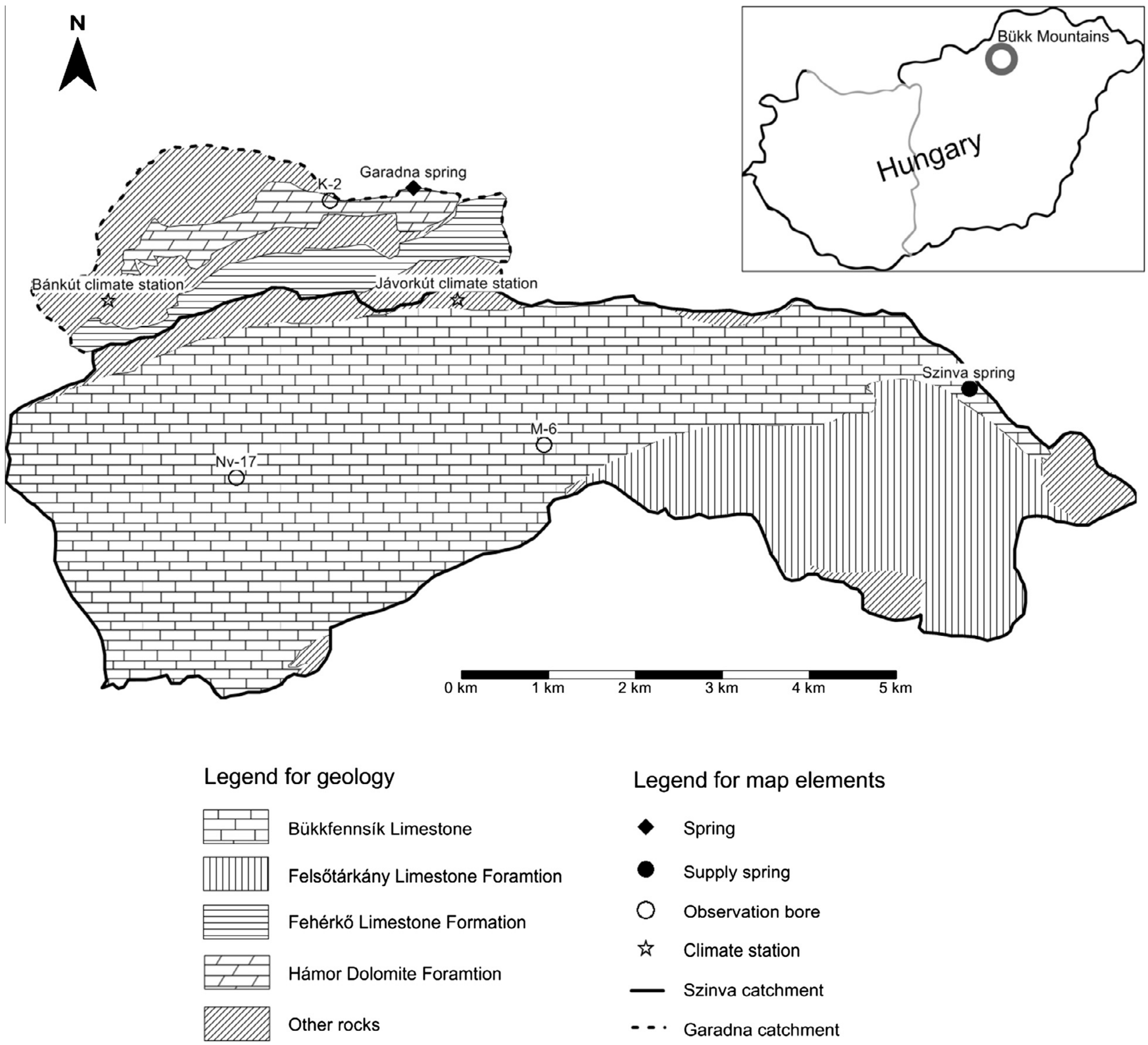

Fig. 5. Geological settings of the Szinva and Garadna catchments.

below the surface outlets of sinkholes. The horizontal distance between supposed karstified zones indicated by sinkholes in the Szinva catchment varies between 200 and 500 m (Fig. 6). The exploration of the Bányász-cave revealed the existence of two or three karstified horizons in the unsaturated zone (Rántó, 2014).

The Szinva spring is located at 340 m ASL. The two observation wells have a ''baseflow'' water level at 522 m ASL (bore NV-17) and 449 m ASL (bore M-6). M-6 is located at 4900 m while Nv-17 is located at 8500 m distance to the West of the Szinva main spring.

7.2. The Garadna catchment

The Garadna catchment is a small catchment adjacent to the much larger Szinva system. The catchment extends over a 1.5 × 4.8 km elongated area of 7.4 km^2 (Figs. 4 and 5). The autogenic recharge area of the spring is equivalent to the surface extent of the Fehérkő Limestone and is estimated to be a 5 × 0.4 km elongated zone. The catchment was delineated based on surface topography, tracing experiments and water budget calculations (Hernádi et al., 2013). The Garadna catchment has a complex geology. It is separated from the neighbouring Szinva catchment by an E-W trending thrust fault. On the northern side of the fault upper-Triassic argillaceous slates extend between the Szinva catchment and the Fehérkő Limestone Formation which is the main recharge area of the Garadna spring. The Fehérkő limestone is well karstified, with an extensive cave system connected to the Garadna spring. Although the Garadna spring is fed by waters infiltrating on the Fehérkő Limestone, the spring itself discharges from Triassic Hámor Dolomite (middle-Triassic platform facies dolomite). The dolomite is separated from the limestone recharge area by a thin strip of metavulcanites. The spring is presumably connected to its recharge area through a conductive fracture passing through the unkarstifiable metavulcanites. Sinkholes are common in the Fehérkő Limestone area, although not as common as in the neighbouring Szinva catchment. The estimated distance between conduit branches based on sinkhole locations and cave maps is approximately 300–500 m.

The Garadna spring is located at 496 m ASL. There is one observation well located in the Garadna surface catchment. The K-2 observation well is drilled into Hámor Dolomite and based on its hydraulic behaviour it is presumed to be hydraulically unconnected to the main recharge area of the spring. The K-2 bore has

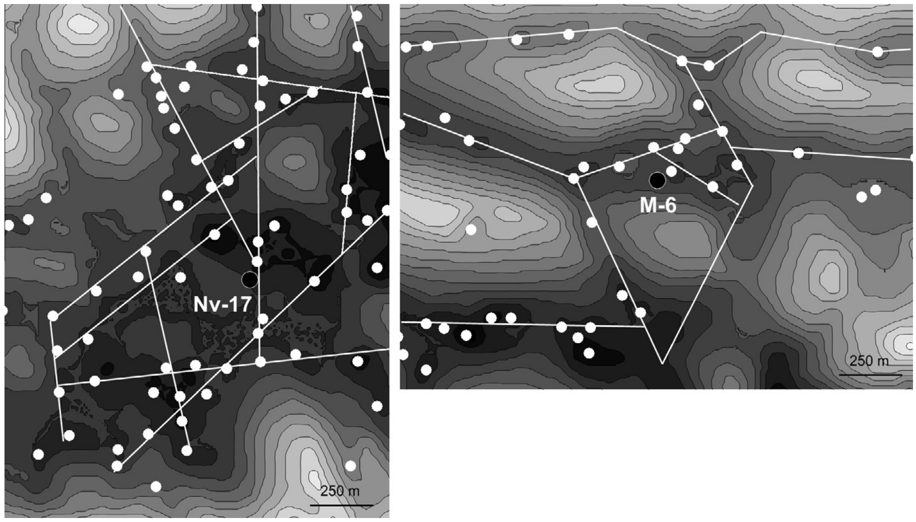

Fig. 6. Sinkhole locations and assumed conduit locations at the Nv-17 and M-6 observation bores of the Szinva catchment. Based on the sinkhole mapping study of Hernádi et al. (2013).

a "baseflow" water level at 524 m ASL. The bore is located at 1000 m distance to the west of the Garadna spring.

7.3. Hydrograph analysis

Hydrographs commonly applied in karst research are usually spring discharge time series which contain hourly data. In this study both discharge data obtained from karst springs and hydraulic head time series obtained from observation wells were applied for parameter estimation. Unlike in statistical analysis of time series, the falling limb of individual hydrograph peaks were analysed (single event models, Kovács and Sauter, 2007). The advantage of single event analysis is that applied methods are based on physical laws and thus it provides quantitative information about the structure, hydraulic parameters, and hydraulic functioning of a system.

7.3.1. Hydrograph data

The hydrographs of monitoring bores Nv-17 and M-6 located on the Szinva catchment, and of K-2 located on the Garadna catchment have been analysed with the aim of deriving information on conduit network geometry. Moreover, the spring hydrographs of the Szinva and Garadna springs were also analysed using hydrograph analytical techniques introduced by Kovács et al. (2005) and Kovács and Perrochet (2008) to obtain information on average block size of these catchments. The present study represents the first physical analysis of hydrograph data obtained in the Bükk area. The specifications of monitoring stations are provided in Table 1.

Throughout the analysis, individual peaks with long recession periods were analysed using the manual decomposition method. Where sufficient data was available, master recession curves were also generated and analysed.

The hydrograph of bore NV-17 includes a 22 year long hourly dataset from 10/10/1992 to 31/01/2014. The bore is screened in Triassic age Bükkfennsík Limestone.

The hydrograph of M-6 is relatively short, including 21 months of daily data. Sporadic hydrograph data is also available for the period between 1995 and 2001. It is possible that this bore intersects with a conduit feature which might explain the sharp flood peak on its hydrograph. It is unclear whether this sharp peak indicates natural processes such as sinkhole recharge, or originates from instrument failure. The bore is screened in Triassic age Bükkfennsík Limestone.

The hydrograph of K-2 includes a 10-month long hourly dataset from 20/06/2013 till 11/04/2014. The bore is screened in the Triassic Hámor Dolomite Formation.

The hydrograph of the Szinva spring consists of a 18-year long daily water level time series. Instead of discharge, water level in a prismatic artificial spring basin was registered. As shown in Eq. (5), water level in such settings follows an exponential behaviour with the same recession coefficient as spring discharge. Consequently, the water level time series of the Szinva was applied for hydrograph analysis.

Table 1
Summary of hydrograph decomposition results. L indicates block size derived using symmetrical assumption and L_x and L_y indicates block dimensions using asymmetric solution. MRC indicates Master Recession Curve results.

Station name	Station type	TOC (mASL)	Bore depth (m)	Screen depth (m)	Total screen length (m)	Screened formation/main aquifer	Instrument depth (m)	Instrument type	Data period	Baseflow SWL (mASL)
NV-17	Bore	780	350	310–331	12	Bükkfennsík Limestone	260	DATAQUA	1992–2014	522
M-6	Bore	723	300	250–275	25	Bükkfennsík Limestone	280	DATAQUA	1995–2001	449
K-2	Bore	560	136	57–124	20	Hámor Dolomite	40	DATAQUA	2013–2014	524
Szinva	Spring	340	N/A	N/A	N/A	Bükkfennsík Limestone	8	DATAQUA	1996–2014	340
Garadna	Spring	496	N/A	N/A	N/A	Fehérkő Limestone	2	DATAQUA, ISCO 2150	1994–2014	496

The hydrograph of the Garadna spring includes a 21-year long daily water level time series. In November 2013 the spring was equipped with an ISCO 2150 type acoustic flow meter, which made the calculation of the level-discharge relationship possible. This flowmeter measures mean flow velocity every 15 min. The instrument has one sensor which uses continuous wave Doppler technology. Water level data is measured by an automated pressure transducer registering also water temperature and conductivity. Discharge was calculated by determining the head-discharge relationship (Szegediné Darabos et al., 2014). The resulting discharge curve is indicated in Fig. 10.

The hydrographs of NV-17, M-6, K-2 and of the Szinva and Garadna Springs are indicated in Figs. 7–11. Thick lines indicate the analysed sections of the hydrographs.

7.3.2. Master recession curves

Master recession curves were constructed from available hydrograph data using two different methods. Master recession curves were assembled for each data series using a manual approach. According to the manual approach, selected segments of the time series were moved on the timeline (horizontal axis), to form one continuous master recession curve. The applied hydrograph segments were selected in comparison with rainfall data, and only undisturbed recession periods were applied, which were preceded by at least 5 days of dry weather.

Hydrographs with insufficient or incomplete data necessary for a manual master recession curve assembling were processed using the strongly hybridised genetic algorithm (Gregor and Malik, 2012). Master recession curves were decomposed and analysed

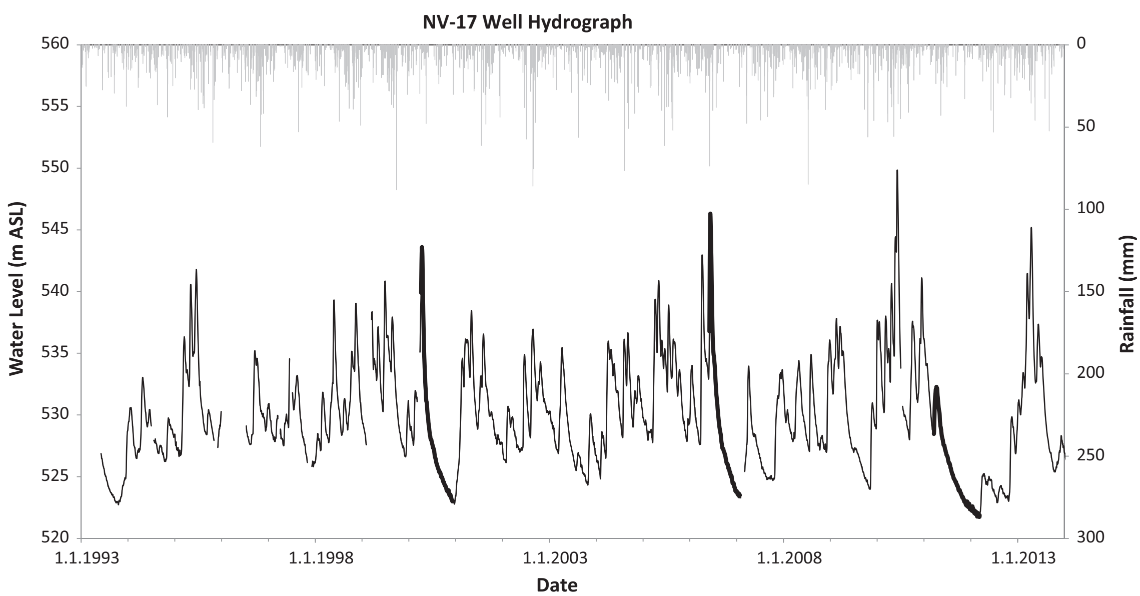

Fig. 7. Hydrograph of well NV-17 for the period of 01/01/1993–01/01/2014.

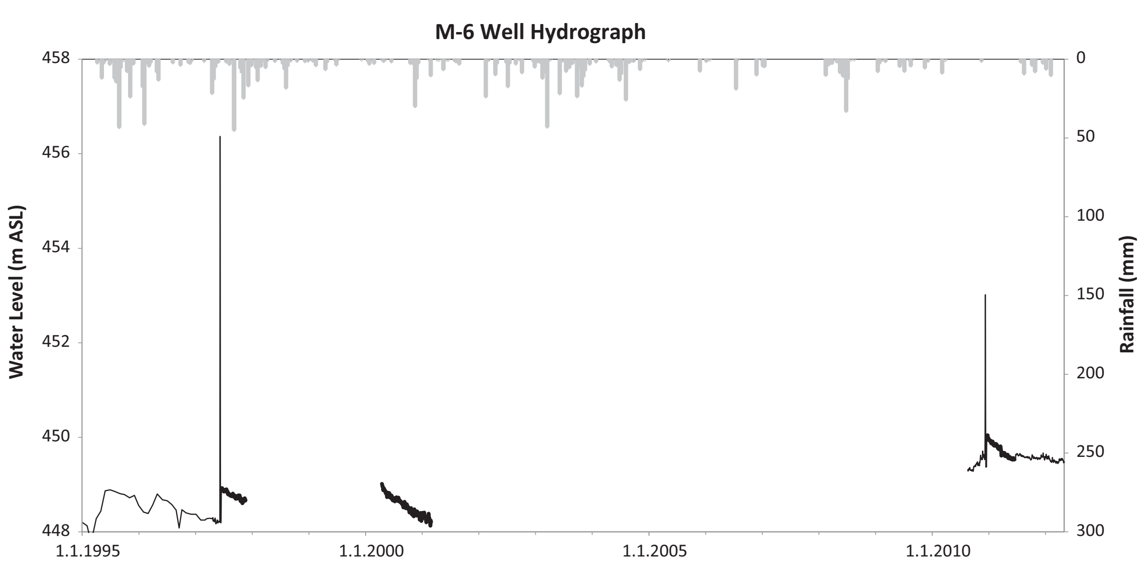

Fig. 8. Hydrograph of well M6 for the period of 01/08/2010–01/05/2012.

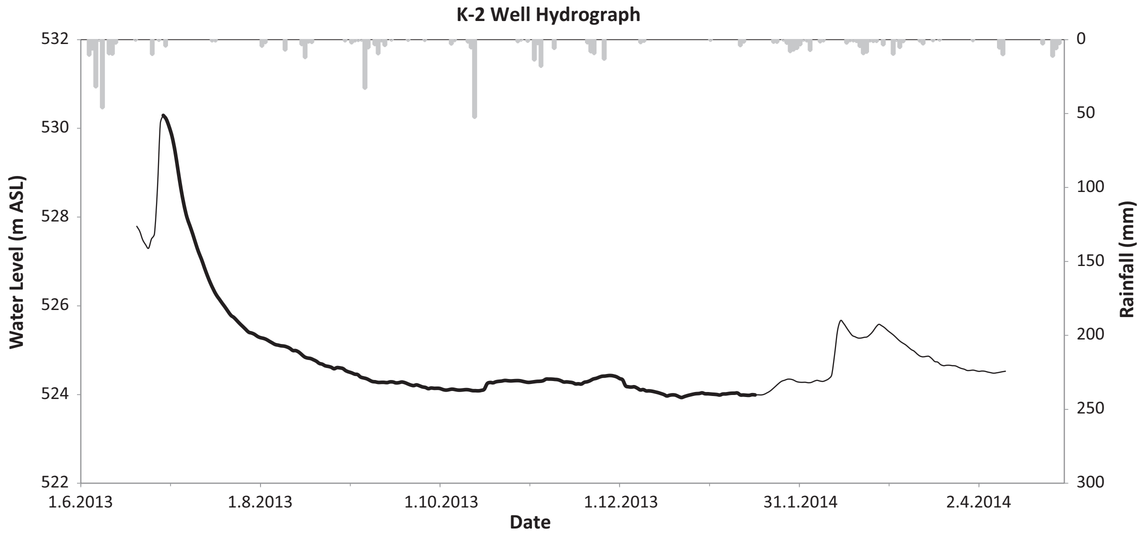

Fig. 9. Hydrograph of well K2 for the period of 20/06/2013–11/04/2014.

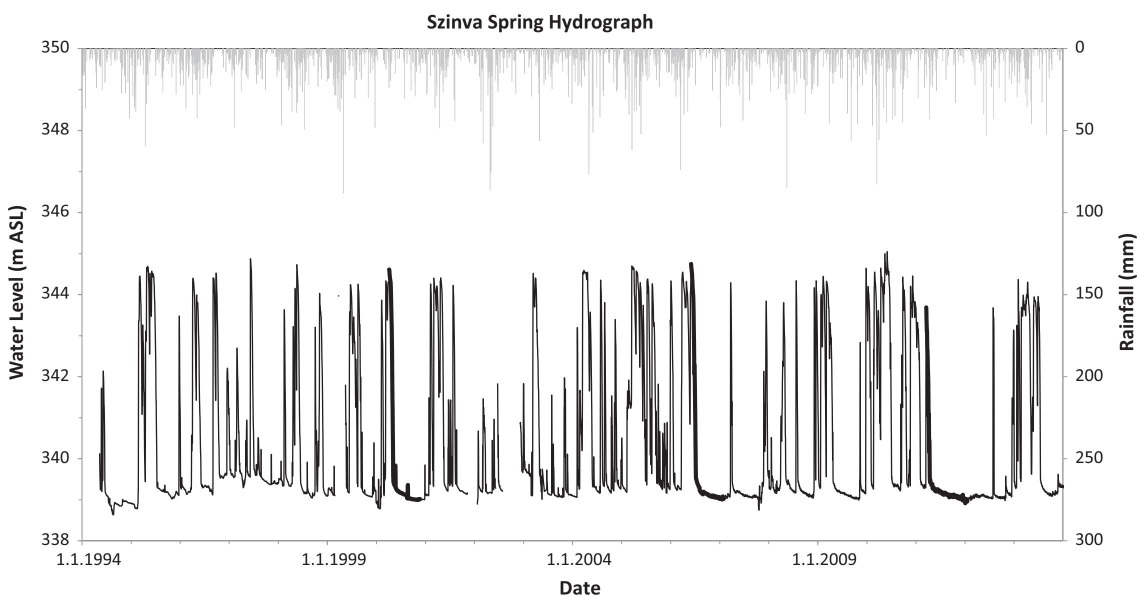

Fig. 10. Hydrograph of the Szinva spring for the period of 12/05/1994–04/11/2014.

together with individual hydrograph peaks to characterise the temporal variability of recession coefficients and to decrease the uncertainty of our analyses. The decomposition of individual peaks and master recession curves gave very similar results (Table 2).

7.3.3. Hydrograph decomposition

The theory of spring hydrograph decomposition was introduced by Forkasiewicz and Paloc (1967). The falling limb of spring hydrograph peaks can usually be decomposed into three exponential segments (see Fig. 12). According to the interpretation of Forkasiewicz and Paloc (1967) the different hydrograph segments correspond to different reservoirs, each contributing to spring discharge. Forkasiewicz and Paloc (1967) identified these reservoirs as the conduit network, an intermediate system of integrated fissures, and a low permeability network of pores and narrow fissures. According to this model, spring discharge can be described by the following formula:

$$Q_{(t)} = Q_1 e^{-\alpha_1 t} + Q_2 e^{-\alpha_2 t} + Q_3 e^{-\alpha_3 t} \quad (18)$$

Kovács and Perrochet (2008) disproved the above interpretation, and showed that hydrographs of homogeneous flow domains can be decomposed into an infinite number of exponential components and that only three of these components contribute significantly to total discharge. The same applies to well hydrographs as demonstrated in Sections 6.1 and 6.2.

The decomposition technique applied in this study includes the manual fitting of exponential curves on semi-log time-water level or time-discharge diagrams using MS EXCEL spreadsheets. After the satisfactory fitting, the fitted exponential function was subtracted from the time series, and a new exponential curve was fitted on the residual values. This process was repeated until reasonable fitting was possible. In most cases two or three exponential could be fitted on data series obtained from our test sites.

While in the case of spring hydrographs the hydrograph components are always positive, in the case of well hydrographs the sec-

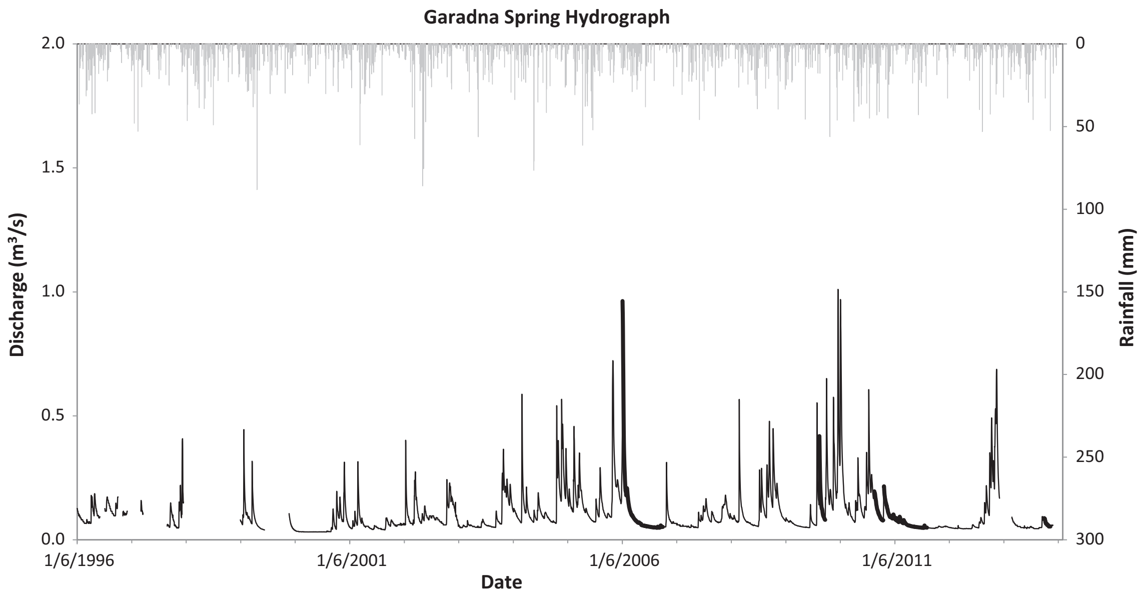

Fig. 11. Hydrograph of the Garadna spring for the period of 01/06/1996–01/01/2014.

Table 2
Specifications of monitoring stations applied.

Station	Period	K (m/s)	Ss (1/m)	α_1 (1/s)	α_2 (1/s)	α_3 (1/s)	γ (−)	β (−)	$L_{catchment}$ (m)	L_{block} (m)	$L_{x\ block}$ (m)	$L_{y\ block}$ (m)
NV-17	MRC	1.00E−05	5.00E−03	5.00E−10	4.00E−07	1.00E−06	0.40	0.48	8886	313	246	513
	06/04/2000–07/12/2000	1.00E−05	5.00E−03	7.00E−10	6.00E−07				7510	256		
	03/06/2006–25/01/2007	1.00E−05	5.00E−03	7.50E−10	5.00E−07	2.00E−06	0.25	0.77	7255	280	251	324
	20/03/2011–11/03/2012	1.00E−05	5.00E−03	5.00E−10	4.00E−07				8886	313		
	Average	1.00E−05	5.00E−03	6.13E−10	4.75E−07	1.50E−06	0.32	0.63	8028	291	241	384
M-6	MRC	1.00E−05	5.00E−03	4.00E−11	3.00E−07				31416	362		
	16/06/1997–19/11/1997	1.00E−05	5.00E−03	5.00E−11					28099			
	16/04/2000–26/02/2001	1.00E−05	5.00E−03	8.00E−11	2.00E−07				22214	443		
	21/12/2010–16/06/2011	1.00E−05	5.00E−03	5.00E−11	1.50E−07				28099	512		
	Average	1.00E−05	5.00E−03	5.50E−11	2.17E−07				26792	439		
K-2	MRC	1.00E−05	5.00E−03	1.00E−10	2.00E−07	2.00E−06	0.10	0.33	19869	443	331	993
	29/06/2013–15/01/2014	1.00E−05	5.00E−03	5.00E−11	7.00E−07	5.00E−06	0.14	0.55	28099	237	192	349
	Average	1.00E−05	5.00E−03	7.50E−11	4.50E−07	3.50E−06	0.12	0.44	22943	340	229	518
Szinva	MRC	1.00E−05	5.00E−03	4.00E−11	6.00E−07				31416	256		
	6/04/2000–23/11/2000	1.00E−05	5.00E−03	7.00E−11	1.00E−06	1.50E−05	0.07	0.65	23748	198	168	257
	03/06/2006–25/01/2007	1.00E−05	5.00E−03	4.00E−11	6.00E−07	2.00E−05	0.03	0.87	31416	256	240	277
	20/03/2011–20/01/2012	1.00E−05	5.00E−03	4.00E−11	6.00E−07	2.00E−05	0.03	0.87	31416	256		
	Average	1.00E−05	5.00E−03	4.75E−11	7.00E−07	1.83E−05	0.04	0.80	28829	242	215	270
Garadna	MRC	1.00E−05	5.00E−03	2.00E−08	2.50E−07		0.08	0.55	1405	397	321	582
	03/06/2006–28/02/2007	1.00E−05	5.00E−03	2.00E−08	3.80E−07	3.00E−06	0.05	0.75	1405	322	284	381
	12/01/2010–19/02/2010	1.00E−05	5.00E−03		2.50E−07					397	281	
	16/01/2011–15/03/2011	1.00E−05	5.00E−03		2.00E−07	1.50E−06				443	314	
	20/03/2011–31/12/2011	1.00E−05	5.00E−03	2.00E−08	1.50E−07	2.00E−06	0.13	0.48	1405	512	402	838
	28/02/2014–25/04/2014	1.00E−05	5.00E−03	5.00E−08		2.00E−06	0.03	0.62	889			
	Average	1.00E−05	5.00E−03	2.75E−08	2.46E−07	2.13E−06	0.07	0.60	1198	414	321	600

ond component (H2 or H4 in Eq. (8)) can equally take negative or positive values depending on x and y. Such situation is indicated by convex hydrograph peak. If the second exponential component (H2) is positive (concave hydrograph peak), the traditional decomposition technique can be applied. In the case if the second exponential component (H2) is negative (convex hydrograph peak), a complementary decomposition approach can be applied. After fitting a straight line on the semi log graph of the "baseflow" well hydrograph, the remaining hydrograph needs to be subtracted from the first exponential. A second exponential can then be determined by curve fitting on the residual hydrograph. In most cases a third exponential can be fitted, which can also be used for parameter estimation purposes.

7.3.4. Parameter estimation

Three to five hydrograph peaks of each time series were analysed, together with the master recession curves which were also decomposed according to the method described above, with the exception of bore K2 where only one peak could be analysed because of the short data series. Recession coefficients of the fitted exponential functions were applied for the estimation of the size of dominant flow domains determined by conduit spacing.

7.3.4.1. Asymmetric block assumption. Where several exponential components could be fitted, block asymmetry and conduit spacing were estimated from well hydrographs using the asymmetric ana-

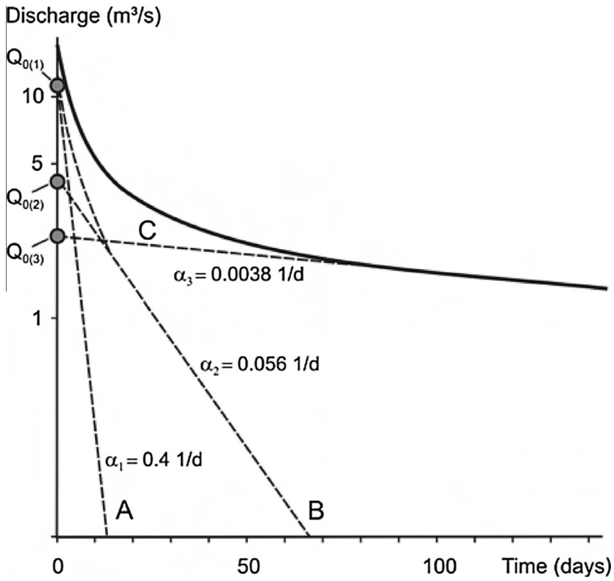

Fig. 12. Decomposition of recession curves according to Forkasiewicz and Paloc (1967).

lytical solution Eq. (8). The asymmetry factor can be estimated from the first two exponentials as follows:

$$\beta = \sqrt{\frac{\gamma - 1}{1 - 9\gamma}} \text{ for } L_y > L_x$$

$$\beta = \sqrt{\frac{9\gamma - 1}{1 - \gamma}} \text{ for } L_x > L_y \tag{19}$$

Or from the first and third exponentials as follows:

$$\beta = \sqrt{\frac{\delta - 1}{1 - 25\delta}} \text{ for } L_y > L_x$$

$$\beta = \sqrt{\frac{25\delta - 1}{1 - \delta}} \text{ for } L_x > L_y \tag{20}$$

where $\gamma = \frac{\alpha_1}{\alpha_2}$, $\delta = \frac{\alpha_1}{\alpha_3}$, α_1, α_2 and α_3 are recession coefficients of the first, second and third exponential components.

In a general situation, where diffuse groundwater flow is directed towards karst conduits during baseflow, the asymmetry factor (Eq. (6)) determined from a well hydrograph provides information on block shape of an individual matrix block. In such situation, the asymmetry factor determined from a spring hydrograph (Kovács and Perrochet, 2008) provides an estimation of average block asymmetry throughout a catchment area, and might be different from the asymmetry factor of individual matrix blocks.

If block asymmetry is estimated via well hydrograph decomposition, and hydraulic tests can be performed in the same or nearby wells, a quantitative estimation of conduit spacing (or block size) can be made from one of the recession coefficients.

$$L_x = \sqrt{\frac{\pi^2 T}{S\alpha_1}(1 + \beta^2)} \tag{21}$$

$$L_y = \frac{L_x}{\beta} \tag{22}$$

7.3.4.2. Symmetric block assumption. Where only one component could be fitted on a hydrograph, block asymmetry was not estimated, instead, conduit spacing was estimated using the symmetric analytical solution Eq. (14). Block size (conduit spacing) can be expressed from the first exponential as:

$$L = \sqrt{\frac{2\pi^2 T}{S\alpha_1}} \tag{23}$$

This method gives an approximate conduit spacing which is in between the actual dimensions of a matrix block in two perpendicular directions. In most cases the symmetric assumption is sufficient for the purpose of an overall understanding of conduit network characteristics and hydraulic behaviour.

8. Results and discussion

The decomposition of well and spring hydrographs analysed are indicated in Figs. 13–17.

The recession coefficients obtained from the decomposition of selected peaks of these hydrographs are summarised in Table 2.

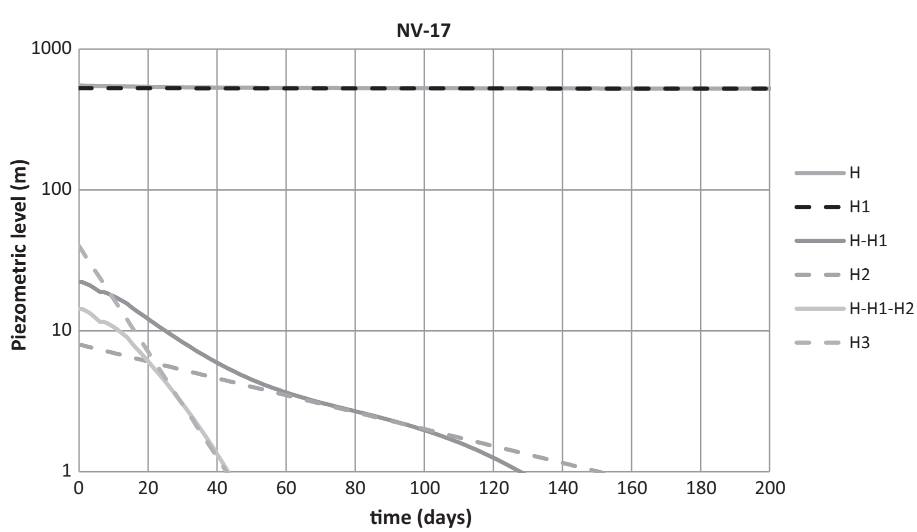

Fig. 13. Decomposition of NV-17 master well hydrograph.

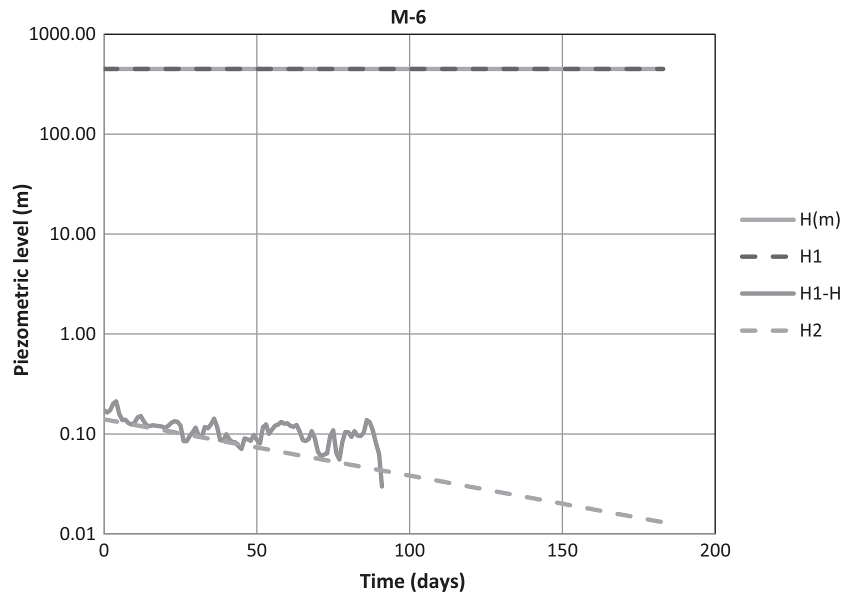

Fig. 14. Decomposition of the M-6 well hydrograph 12/2010–22/06/2011 section.

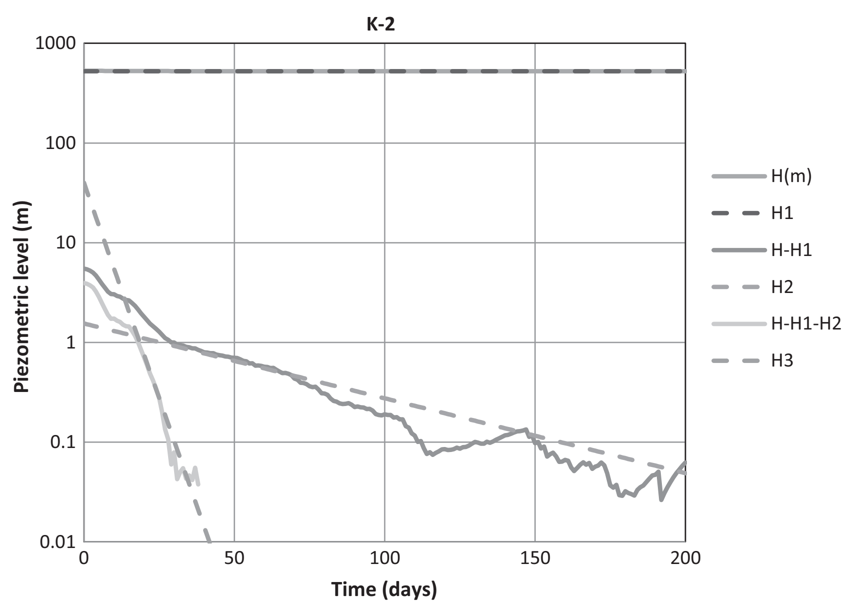

Fig. 15. Decomposition of K-2 master well hydrograph.

The analysis was undertaken according to the formulae introduced in the previous section.

The average value of hydraulic conductivity of the carbonate aquifer matrix determined from recovery well tests is 1e−5 m/s (Székely et al., 2015). A value of 5e−3 was used in our calculations for specific yield of the low permeability rock matrix based on well test data.

Decomposition results indicate the following:

- Three distinct ranges of recession coefficient could be identified on the hydrographs analysed:
  - α_1 ranges between $4.00 \cdot 10^{-11}$ and $5.00 \cdot 10^{-8}\ s^{-1}$;
  - α_2 ranges between $1.50 \cdot 10^{-7}$ and $1.00 \cdot 10^{-6}\ s^{-1}$;
  - α_3 ranges between $1.00 \cdot 10^{-6}$ and $2.00 \cdot 10^{-5}\ s^{-1}$.
- The recession coefficient of the first component (α_1) of the monitoring stations is two to three orders of magnitude lower than the second recession coefficient α_2. This significant difference between α_1 and α_2 cannot be explained by the diffusive emptying of the same aquifer volume. According to the symmetrical analytical solutions (Eq. (14)), it is expected that in general for symmetric blocks $\alpha_2 = 5{\cdot}\alpha_1$. According to the asymmetric solution (Eq. (8)), in the case of an extreme asymmetry of 1:10, the proportion between recession coefficients should be $\alpha_2 = 8.92{\cdot}\alpha_1$. Consequently, during the recession of a homogeneous aquifer block, the difference between α_1 and α_2 remains within one order of magnitude under natural conditions.
- The calculation of block size from recession coefficients for each observation station indicated that the baseflow component (α_1) of the hydrographs reflects the drainage of an extensive aquifer

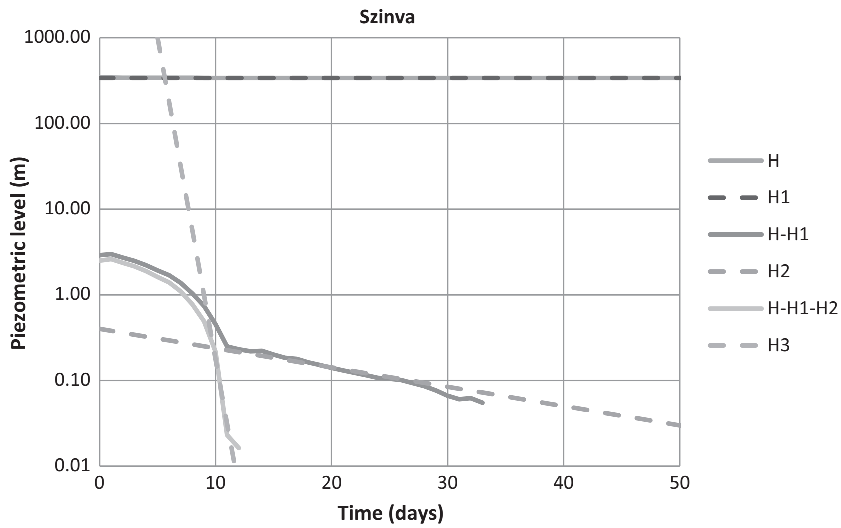

Fig. 16. Decomposition of the Szinva spring hydrograph 03/06/2006–23/07/2006 section.

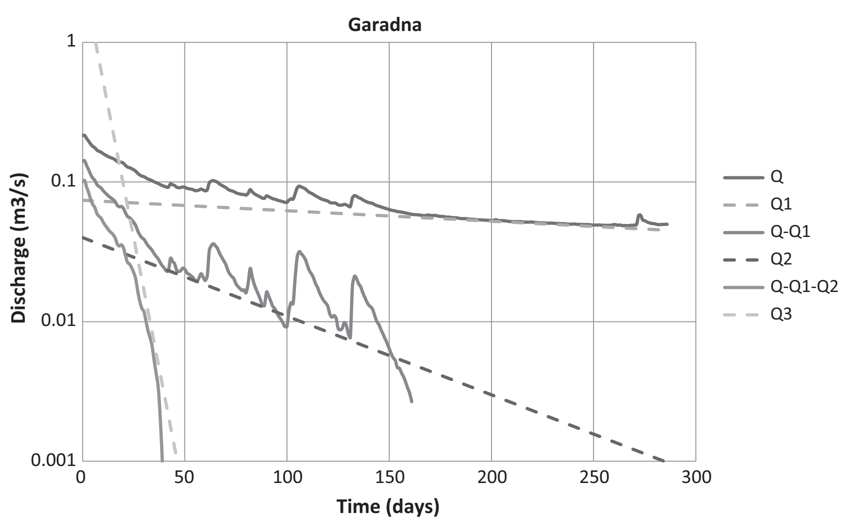

Fig. 17. Decomposition of the Szinva spring hydrograph 20/03/2011–31/12/2011 section.

area ($L \sim 20$ km). The intermediate and flood components (α_2 and α_3) indicate the drainage of low-permeability matrix blocks having a size between $L \sim 200$–500 m.

It is concluded, that after the emptying of the upper karstified zone of the aquifer (α_2 and α_3), water level falls below the level of the main karst conduits, and a much slower drainage of unkarstified limestone zone starts to dominate the recession process (Fig. 18). This process can be characterised with an orders of magnitude lower recession coefficient (α_1). As a consequence, the geometric properties of the matrix blocks can be calculated from the second and third exponentials (α_2 and α_3), while the size of the flow domain under late baseflow conditions can be calculated from α_1. It is important to note, that domain size L in this case is larger than catchment size, as it extends in between two boundary (discharge) zones by definition. In a theoretical symmetrical case, domain size L equals twice the catchment size.

- α_1 shows a large variation, while α_2 is practically the same for each monitoring station. As the α_2 recession coefficient which is representative of block geometry, and estimated average block sizes are similar among all stations of the catchment, any significant variation in hydraulic properties among these aquifer volumes is unlikely. Variations in hydraulic properties at different observation stations might cause inaccuracies in estimated block sizes. These inaccuracies are believed to be within the accuracy expected in this demonstration study. A higher accuracy could be achieved through systematic hydraulic testing and the installation of additional monitoring bores, which was not within the scope of this study.
- α_1 of the Garadna spring is three orders of magnitude higher than that of other stations. This can be explained by the small size of the Garadna catchment. The Garadna spring has an autogenic recharge area of approximately 500 $\times$ 3000 m. Analytical calculations gave $L = 1200$ m for domain size, which is in good accordance with the delineated catchment size. Based on the high value of baseflow coefficient, it seems that this catchment is hydraulically disconnected from the carbonate mass of the uplands area. The reason for the hydraulic isolation is presumably the enclosed position of the Fehérkő Limestone block in between a thrust fault structure and argillaceous slates (Vesszősi Formation) in the South and tight metavulcanite rocks in the North.

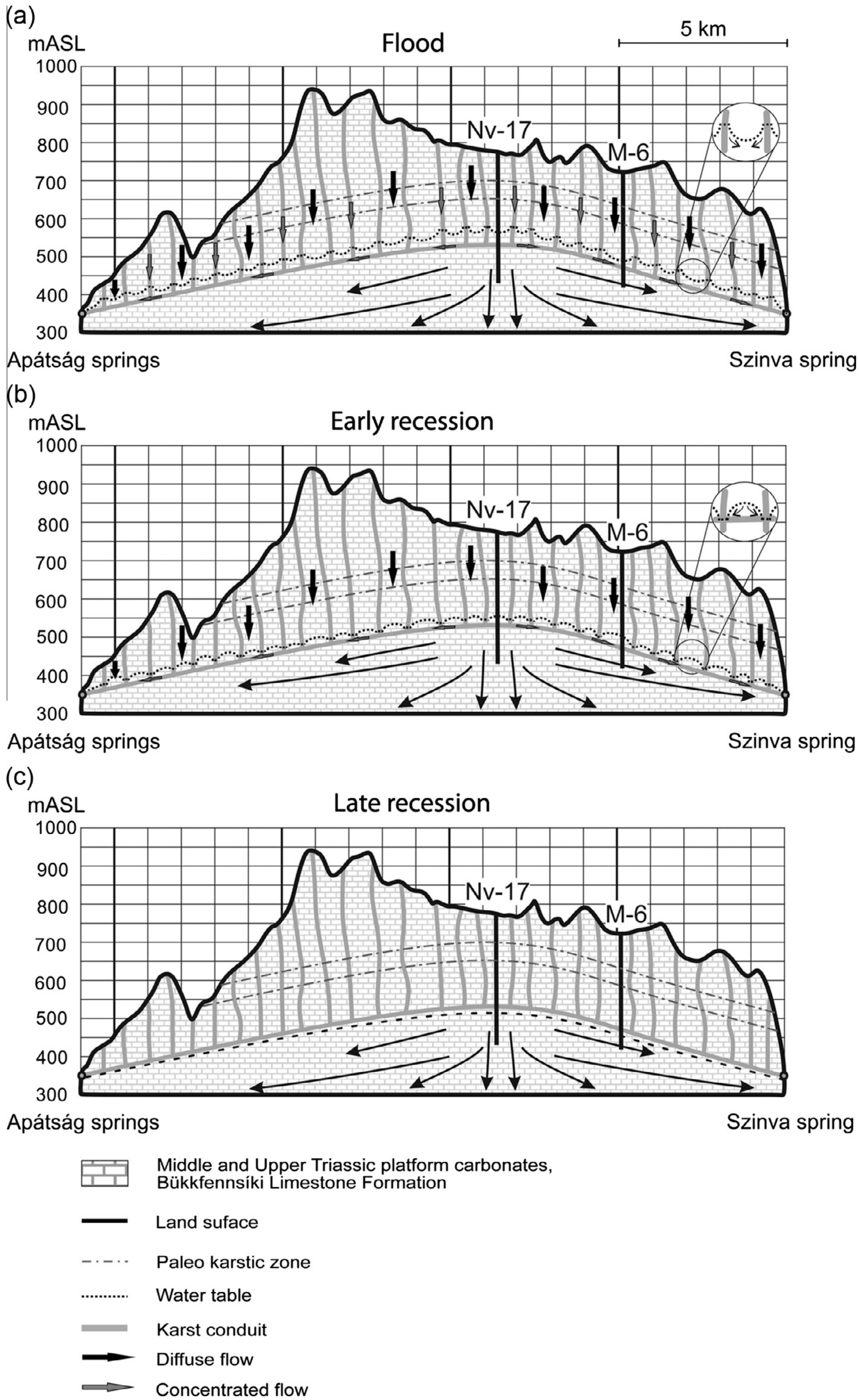

Fig. 18. Conceptual hydrogeological model of the Bükk uplands aquifer system along the A–B cross section indicated in Fig. 4. During flood conditions karst springs are fed by concentrated and diffuse recharge through the conduit network (a). During early baseflow the emptying of matrix blocks feeds karst springs (b). Under drought conditions (late recession) water level drops below the active karstified horizon and large-scale diffuse flow dominates the system (c).

Interestingly, α_1 of monitoring bore K-2 equals to the baseflow recession coefficient of other stations which indicates a hydraulic connection of this bore with the plateau during late baseflow conditions. The K-2 bore is screened in Hámor Dolomite which is presumed to be hydraulically connected to the plateau based on this observation.

- α_1 of monitoring well NV-17 is one order of magnitude lower than that of other stations. It is presumed, that the position of the catchment boundary of the Szinva catchment compared to this bore is uncertain. It cannot be excluded, that during late baseflow conditions NV-17 belongs to one of the neighbouring smaller catchments such as the Jávor-kút (N), Garadna (N), Csipkés-kút (N), Bán-kút (NW), Csurgó-kút (NW), or Imókő (SW) spring catchments. Dye tracing can be applied to assign this bore to the appropriate catchment in the future.

- Calculated late recession domain size (22–28 km) for most monitoring stations is in accordance with the size of the entire Bükk carbonate plateau (20 km). Based on this observation it is presumed, that during drought (late baseflow) conditions the majority of the carbonate plateau behaves as a hydraulically interconnected single-continuum domain discharging into bordering valleys and karst springs. Hydrograph analysis indicated, that in this flow regime the water table conduit network becomes inactive and diffuse flow dominates the system.
- In the case of the M-6 monitoring bore, the third exponential could not be determined properly because of insufficient data, and thus only the symmetrical solution was applied in our calculations.

9. Conclusions

The present paper describes a quantitative methodology for the estimation of hydraulic and geometric parameters of karst systems from well and spring hydrograph data. New analytical solutions for the spatio-temporal variation of hydraulic potentials in rectangular matrix blocks were introduced. Besides the description of new parameter estimation tools, a detailed field application of these methods was presented.

As spring hydrograph data is not always available, well hydrographs represent an alternative way to hydraulic parameter estimation. Spring hydrograph analytical methods assume a uniform parameter distribution and conduit spacing throughout a karstic catchment, and thus provide information on average hydraulic properties and conduit network geometry. This information is crucial for groundwater modelling purposes. Well hydrographs facilitate to determine the size and hydraulic parameters of matrix blocks at specific locations. This information is useful for characterising spatial variability, to characterise local hydraulic properties and to localise karst features. The combination of the spring and well hydrograph analytical techniques provides a powerful tool for the characterisation of the structure and hydraulic properties of karst systems.

Recession coefficient is an important indicator of block geometry and hydraulic characteristics. In most cases well hydrograph peaks can be decomposed into three exponential segments reflecting the diffusive emptying of matrix blocks. More than an order of magnitude difference between the recession coefficients of exponential components of a well or spring hydrograph is interpreted to indicate scale change of groundwater flow.

Hydrograph analysis of three well hydrographs and two spring hydrographs from two adjacent karstic catchments (Szinva and Garadna) located in the Bükk Mountains, North-East Hungary was undertaken to demonstrate the applicability of the introduced methodology. The analysis of well hydrographs provided similar results to spring hydrograph analysis. Three distinct ranges of recession coefficient could be identified on the hydrographs analysed. The significant difference between recession coefficients indicated the change of flow scale during the recession process.

Based on hydrograph analysis it was concluded, that the flow system is dominated by diffuse flow inside matrix blocks and concentrated flow within the conduit network during flood recession and early baseflow recession. During late baseflow recession the water level drops below the karstified horizon, concentrated flow ceases within karst conduits, and large scale diffuse flow starts to dominate the system.

The spring hydrograph of the Garadna spring indicates that this catchment is hydraulically isolated from the main carbonate plateau of the Bükk uplands area.

Block sizes determined from well and spring hydrographs range between 200 and 500 m. A block asymmetry of $L_x/L_y = 0.3–0.8$ was determined from hydrograph data. These values were in agreement with field observations.

Acknowledgements

Part of this research was carried out at the Sustainable Resource Management Center of Excellence at the University of Miskolc, as part of the TÁMOP-4.2.2/A-11/1-KONV-2012-0049 "WELL aHEAD" project in the framework of the New Széchenyi Plan, funded by the European Union, co-financed by the European Social Fund.

We would like to thank Béla Hernádi for sharing his field experience at the test site.

References

Atkinson, T.C., 1977. Diffuse flow and conduit flow in limestone terrain in the Mendip Hills, Somerset (Great Britain). J. Hydrol. 35, 93–103.

Bagarić, I., 1978. Determination of storage and transportation characteristics of karst aquifers. In: Milanović, P.T. (Ed.), Karst Hydrogeology. Water Resources Publications, Littleton, CO, USA (434 p, 1981).

Berkaloff, E., 1967. Limite de validité des formules courantes de tarissement de débit. Chronique d'Hydrogéol. 10, 31–41.

Böcker, T., 1969. Az első karsztvíz megfigyelőkút a Bükk hegységben. Hidrol. Tájékoztató, 108–109.

Böcker, T., Vecsernyés, Gy., 1983. Miskolc város vízellátására foglalt karsztforrások védıidomának víz-és környezetvédelmi atlasza. Hungalu, Budapest.

Carslaw, H.S., Jaeger, J.C., 1959. Conduction of Heat in Solids, second ed. Oxford University Press, London, pp. 144 and 173.

Darabos, E., 2010. Examining relationships in data recorded with the Bükk Karst Water Monitoring System. Karst Develop. 1 (1), 6–12, ISSN: 1585–5473.

Darabos, E., Szűcs, P., Németh, Á., 2012. Application of the ACE algorithm on hydrogeological monitoring data from the Bükk Mountains. Acta Geodaet. Geophys. Hung. 47 (2), 256–270 (ISSN: 1217–8977) (eISSN: 1587–1037).

Dataqua, 2002. DATAQUA Elektronikai Kft – Tájékoztató füzet, Balatonalmádi, Hungary.

Dombi, S., 1766. In: Imre Felix, Bader (Ed.), Relatio de mineralibus inclyti Comitatus Borsodiensis aquis facta ad excelsum consilium regium locumtenentiale. Vindobonae, 23 p.

Forkasiewicz, J., Paloc, H., 1967. Le régime de tarissement de la Foux-de-la-Vis. Etude préliminaire. Chronique d'Hydrogéol. BRGM 3 (10), 61–73.

Gondár-Sőregi, K., Gondár, K., Székvölgyi, K., Kun, É., Simonffy, Z., Ács, T., Tahy, Á. 2011. Climate Change and Impacts on Water Supply. Bükk Mountains Test Area. CC-WaterS project, European Regional Development Fund (ERDF), 51 p.

Gregor, M., Malik, P., 2012. Construction of master recession curve using genetic algorithms. J. Hydrol. Hydromech. 60 (1), 3–15.

Hernádi, B., Balla, B., Czesznak, L., Horányi-Csiszár, G., Sűrű, P., Tóth, K., 2013. Felszíni és felszínalatti (barlangi és töbörvizsgála-tok) valamint a Bükki karsztvízszint észlelő rendszer (BKÉR) adatainak térinformatikai rendszerbe történő szervezése. A Magyar Hidrológiai Társaság XXXI. Országos Vándorgyűlése, Gödöllő.

Király, L., Morel, G., 1976. Remarques sur l'hydrogramme des sources karstiques simule par modeles mathematiques. Bull. d'Hydrogéol. Neuchatel 1, 37–60.

Király, L., 2002. Karstification and groundwater flow. In: Proceedings of the Conference on Evolution of Karst: From Prekarst to Cessation. Postojna-Ljubljana, pp. 155–190.

Kessler, H., 1955. Der Versickerungsbeiwert in Karstgebieten. (A beszivárgási százalék karsztvi-dékeinken). Wasserwirtschoft-Wassertechnik, Berlin, vol. 5, no. 12, pp. 392–395.

Kessler, H., 1959. Az országos forrásnyílvántartás. VITUKI, Budapest.

Kovács, A., 2003a. Geometry and Hydraulic Parameters of Karst Aquifers: A Hydrodynamic Modeling Approach. Doctoral Thesis, University of Neuchâtel, Switzerland, 131 p.

Kovács, A., 2003b. Estimation of conduit network geometry of a karst aquifer by means of groundwater flow modelling (Bure, Switzerland). Boletin Geol. Minero 114 (2), 183–192.

Kovács, A., Perrochet, P., Király, L., Jeannin, P.-Y., 2005. A quantitative method for the characterization of karst aquifers based on spring hydrograph analysis. J. Hydrol. 303, 152–164.

Kovács, A., Perrochet, P., 2008. A quantitative approach to spring hydrograph decomposition. J. Hydrol. 352, 16–29.

Kovács, A., Sauter, M., 2007. Modelling karst hydrodynamics. In: Goldscheider, Nico, Drew, David (Eds.), Methods in Karst Hydrogeology. International Contribution to Hydrogeology, Series 26, pp. 201–222 (ISBN: 13: 978-0-415-42873-6).

Kovács, A., Perrochet, P., 2014. Well hydrograph analysis for the estimation of hydraulic and geometric parameters of karst aquifers. In: Mudry, J., LaMoreaux, J.W. (Eds.), H2Karst Research in Limestone Hydrogeology. Environmental Earth Sciences Book Series. Springer Science and Business Media, Heidelberg, pp. 97–114.

Lénárt, L., 2005. Some Aspects of the "3E's" (Economics-Environment-Ethics) Model for Sustainable Water Usage in the Transboundary Slovakian and Aggtelek Karst Region Based on Some Examples from the Bükk Mountains. PhD Thesis Work, Kassa/Kosice.

Lénárt, L., 2010. The interaction of cold and warm karst systems in the Bükk region. In: Proceedings of the 1th Knowbridge Conference on Renewables, Miskolc, pp. 111–118.

Lénárt, L., Hernádi, B., Szegediné Darabos, E., Debnár, Zs., Czesznak, L., Tóth, M., 2014. The importance of Bükk Karst Water Monitoring System (BKWMS) in researching the relations of cold and warm karst waters in the area. Geosciences and Engineering: A Publication of the University of Miskolc, vol. 3, no. 5, pp. 107–117 (ISSN: 2063–6997).

Maillet, E. 1905. Essais d'hydraulique souterraine et fluviale. Hermann, Paris.

Powers, J.G., Shevenell, L., 2000. Evaluating transmissivity estimates from well hydrographs in karst aquifers. Ground Water 38 (3), 361–369.

Pelikán, P., 2005. A Bükk hegység földtana. MÁFI kiadvány.

Rorabough, M.I., 1960. Use of water levels in estimating aquifer constants in a finite aquifer. Int. Assoc. Sci. Hydrol. 52, 314–323.

Rorabaugh, M.I., 1964. Changes in Bank Storage. Publication No. 63, IASH, Gentbrugge, pp. 432–441.

Rántó, A., 2014. A Bányász-barlang kutatása 2014-ben. <http://www.termeszetvedelem.hu>.

Sásdi, L., Less, G.Y., Pelikán, P., 2002. A Bükk karsztvíztározó összleteinek térbeli lehatárolása. In: Karsztvízkutatás Magyarországon II. A bükki karsztvízkutatás legújabb eredményei. Miskolc, pp. 7–13.

Shevenell, L., 1996. Analysis of well hydrographs in a karst aquifer: estimates of specific yields and continuum transmissivities. J. Hydrol. 174, 331–355.

Szegediné Darabos, E., Miklós, R., Tóth, M., Lénárt, L., 2014. Hydrogeological investigation of the Garadna catchment area. Geosciences and Engineering: A Publication of the University of Miskolc, vol. 3, no. 5, pp. 119–127 (ISSN: 2063–6997).

Székely, F., Szűcs, P., Zákányi, B., Cserny, T., Fejes, Z., 2015. Comparative analyses of pumping tests conducted in layered rhyolitic volcanic formations. J. Hydrol. 520, 180–185.

Worthington, S., 2009. Diagnostic hydrogeologic characteristics of a karst aquifer (Kentucky, USA). Hydrogeol. J. 17 (7), 1665–1678.